

Acoustic Particle Velocity Applications

In-situ Surface Impedance and Reflection Coefficient Method

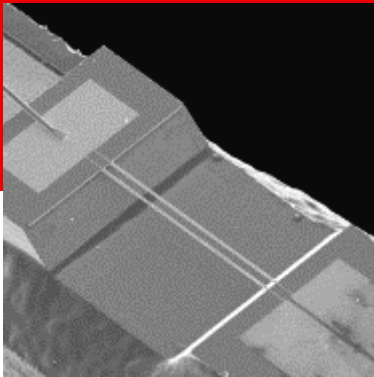
Graciano Carrillo Pousa

carrillo@microflown.com



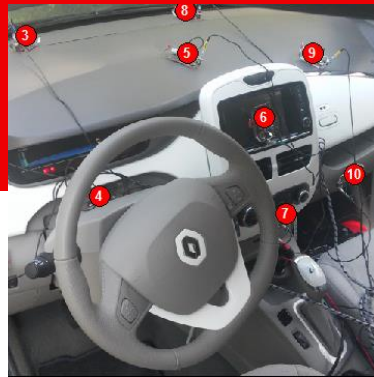
CONTENT

1



Introduction to
particle velocity

2



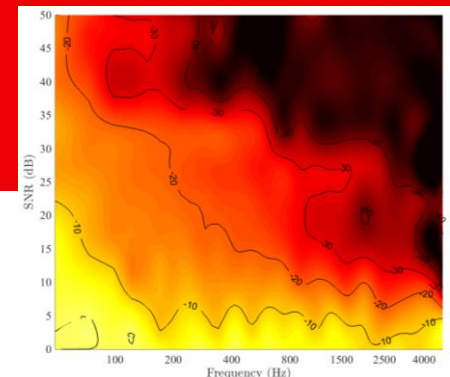
Practical applications

3



In-Situ absorption
estimation based on
Equivalent Source
Method

4



Results and
discussion

A grayscale micrograph of a microfluidic chip. The chip features a grid of rectangular channels. A bright, thin laser beam is directed at the chip from the bottom right, creating a sharp shadow and highlighting the surface texture. The background is black.

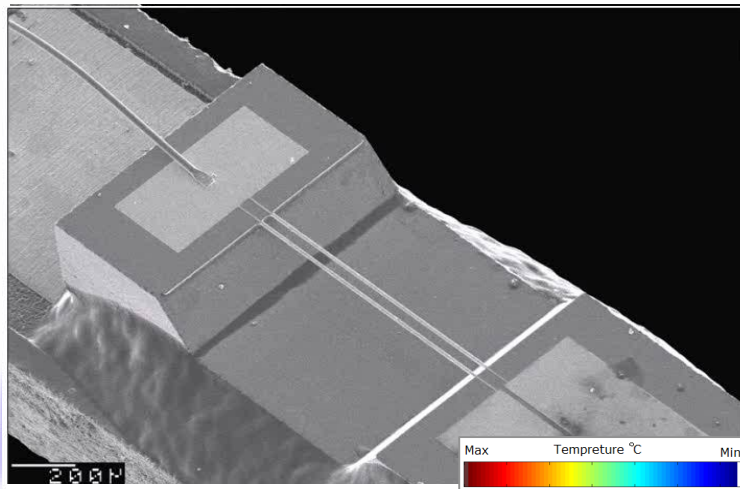
1

INTRODUCTION

Microflow sensor technology

THE MICROFLOWN SENSOR

Measuring particle velocity



1. Two platinum wires heated up to appr. 200 °C
2. As the air flows through the upstream wire, air temperature increases and the wire cools down.
3. Next, the heated air flows through the downstream wire, again the temperature of the wire drops. However, the decrease is lower than it was with the first wire.
4. The different temperatures of the wires cause different electronic resistances. Finally, the resulting voltage difference over the two wires is measured.

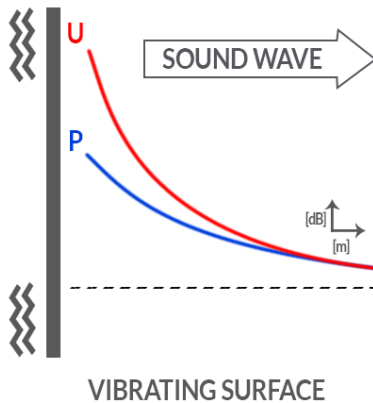
PRESSURE vs PARTICLE VELOCITY

Fundamental physical differences between the two quantities

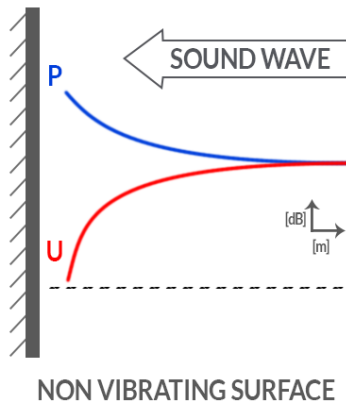
Near field effect

$$\begin{cases} p(r, k) = \frac{A}{r} e^{-jkr} \\ u_r(r, k) = -\frac{1}{j\omega\rho} \frac{\partial p(r, k)}{\partial r} = \frac{p(r, k)}{\rho c} \left(1 + \frac{1}{jkr}\right) \end{cases}$$

$$BC \begin{cases} p^{in} + p^{out} = 0 \\ u_n^{in} - u_n^{out} = 0 \end{cases}$$



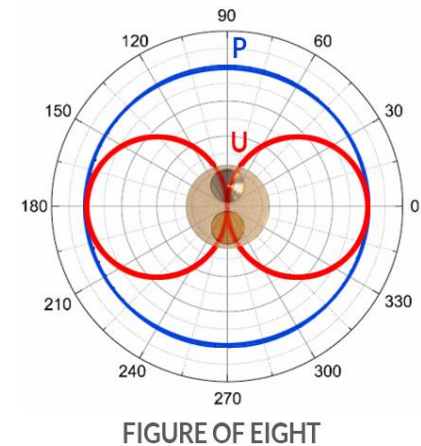
High surface velocity
and low surface pressure



Low surface velocity
and high surface pressure

Figure of 8

$$u_n = \vec{u} \cdot \vec{n} = |\vec{u}| |\vec{n}| \cos(\theta)$$

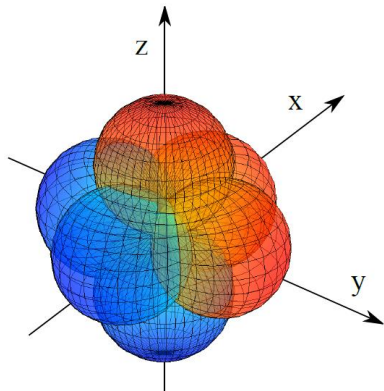


Automatically reduces
the energy received by 1/3

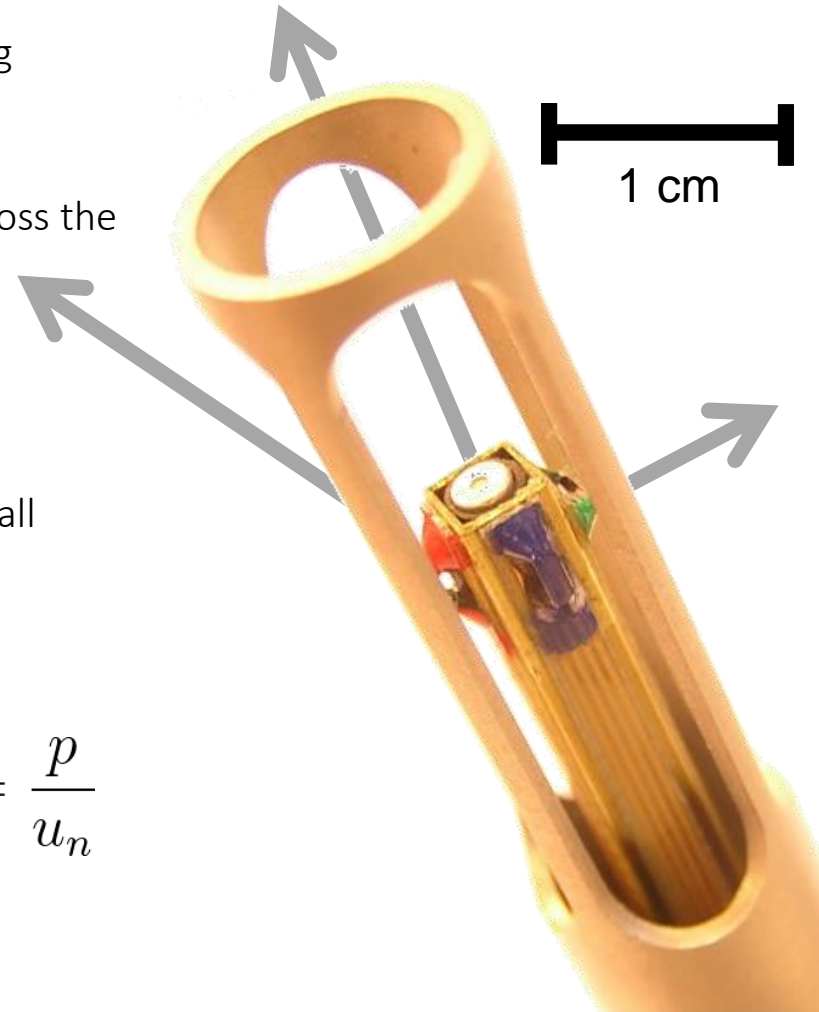
3D ACOUSTIC VECTOR SENSOR

Pressure and particle velocity in the X, Y and Z axis

- Acoustic vector sensors (AVS) can be created by using multiple orthogonal particle velocity sensors
- Localization resolution and accuracy is preserved across the frequency spectrum.
- Broad-banded response | 20 Hz- 20+kHz
- Sound intensity can be obtained by combinations of all sensor elements



$$\vec{I} = \frac{1}{2} P \vec{U}^* \quad Z_n = \frac{p}{u_n}$$



A grayscale micrograph of a microfluidic chip. The chip features a grid of rectangular channels. A bright, thin laser beam is directed at the chip from the bottom right, creating a sharp shadow and highlighting the surface texture. The background is black.

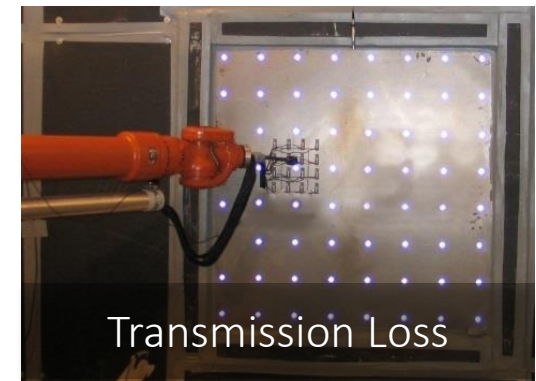
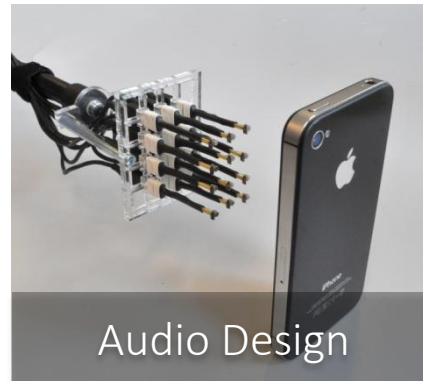
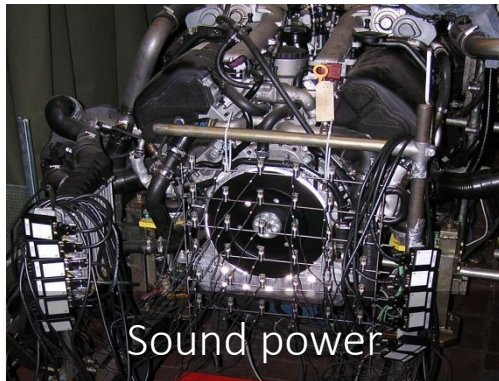
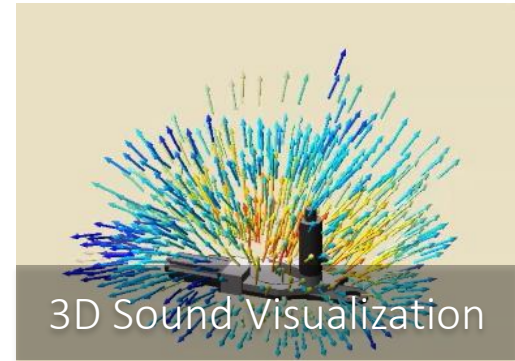
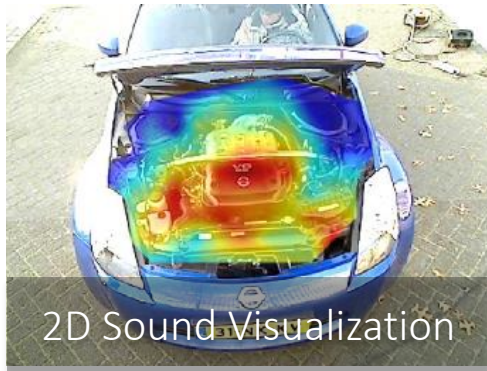
2

Practical applications

Microflow sensor technology

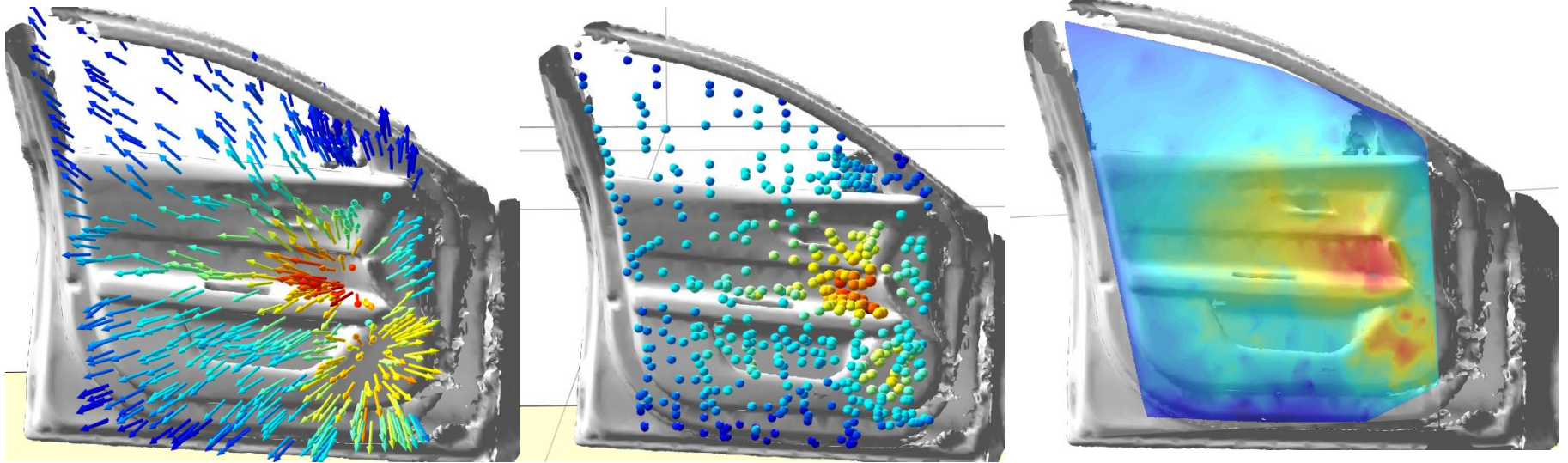
Sensor Applications

Examples of customer applications



SOUND FIELD VISUALIZATION

Analyze results in vector view, scalar view or create as many 2D sound field slices



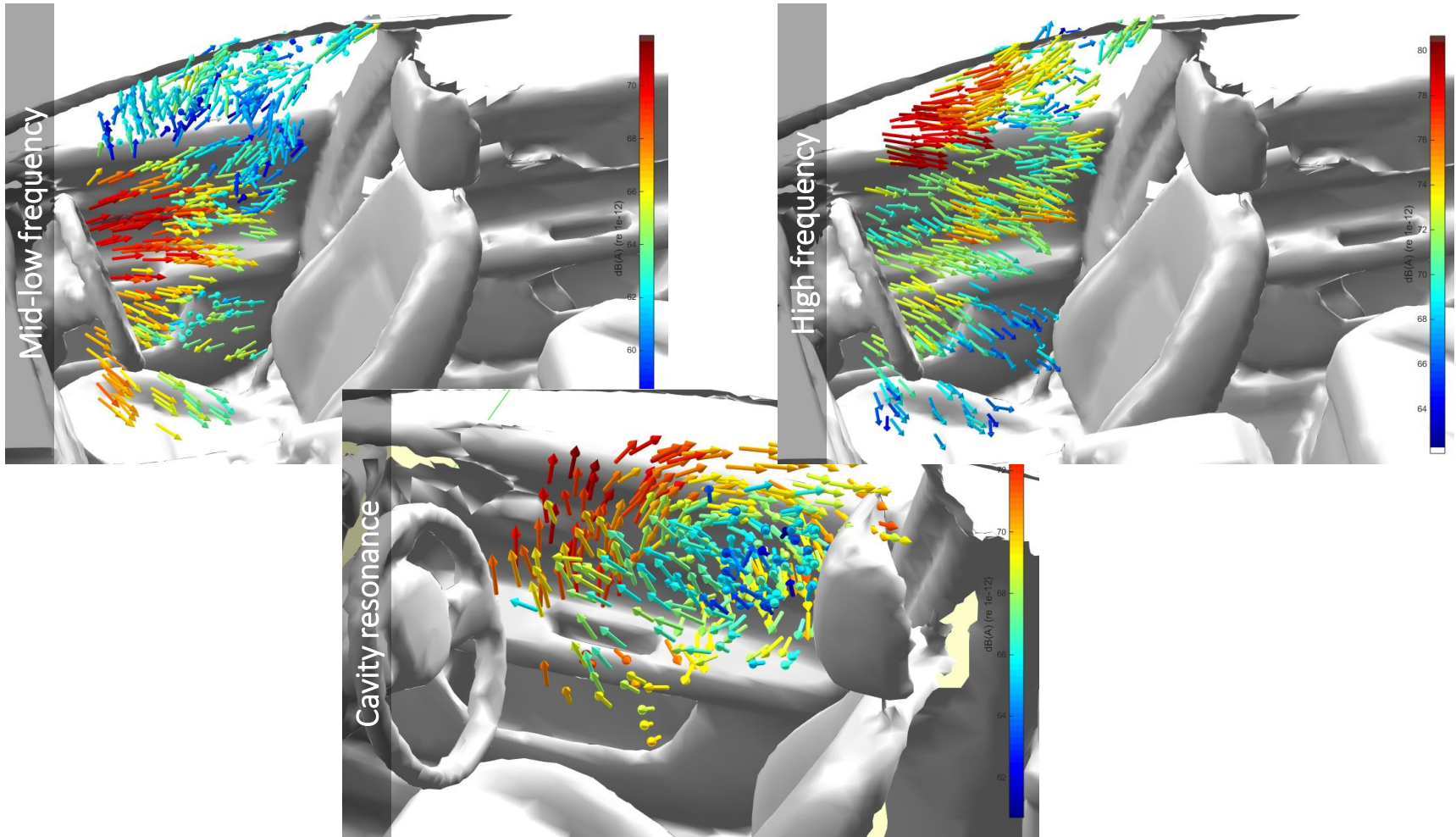
- Vector field

- Sound pressure

- Sound field slices

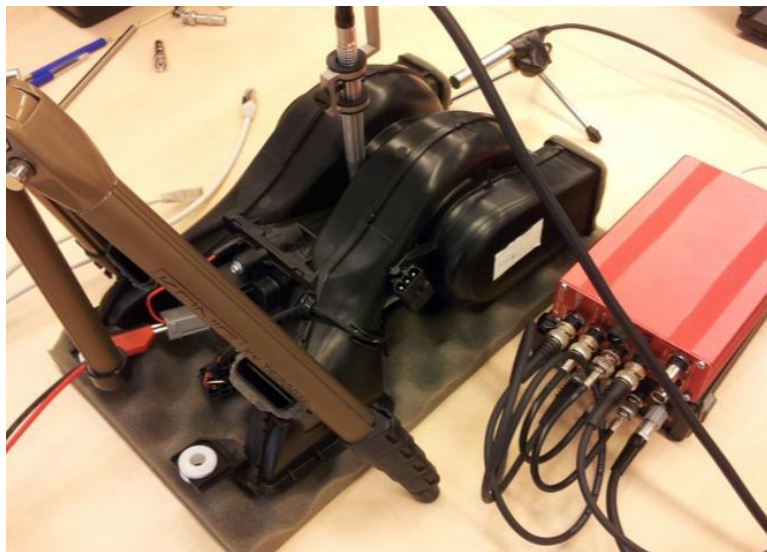
AUTOMOTIVE // AUDIO SYSTEM

Sound visualization around the driver's seat



End of Line // ML Fault Detection

Perform End-of-Line noise tests for objective evaluation, eliminating the variability of the subjective human perception



Measuring in the particle velocity in the near field allows vibro-acoustic characterization in a noisy environment.

MEASUREMENT METHODOLOGY: ORDER TRANSFORM

Velocity Synchronous Discrete Fourier Transform (VSDFT)

$$X(f) = \int_{-\infty}^{+\infty} x(t) e^{-j2\pi f t} dt$$

Domain

$$X(\Omega) = \int x(t) \omega(t) e^{-j\Omega \phi(t)} dt$$

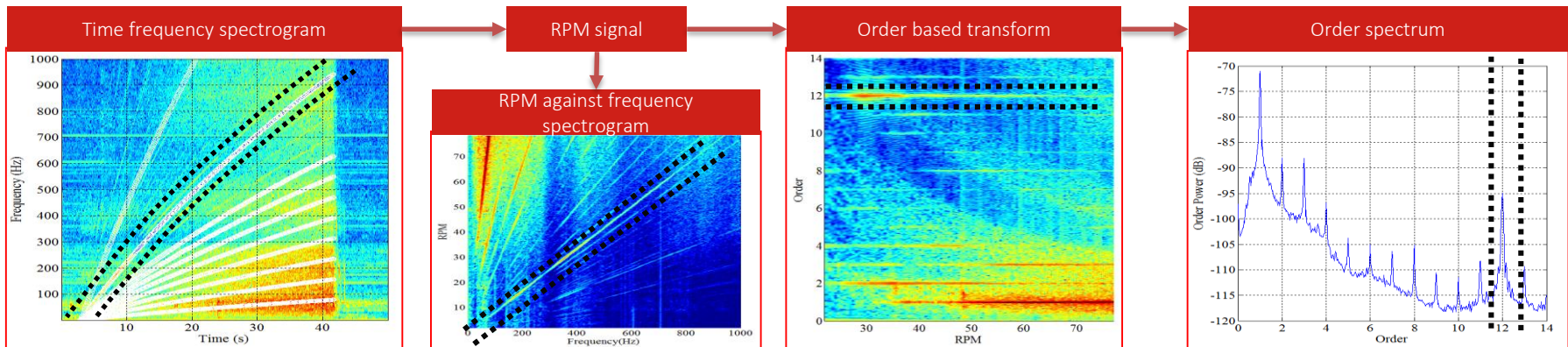
Complex Exponential with RPM related variation

$$\text{VSDFT}[k] = \frac{\Delta t}{\Theta} \sum_{n=0}^{N-1} x[n\Delta t] \omega[n\Delta t] e^{-j\Omega[k\Delta\Omega] \phi[n\Delta t]} dt$$

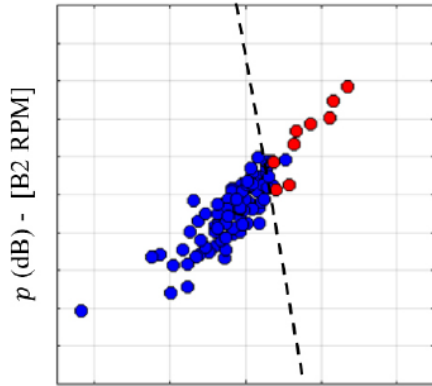
Fourier Transform

Order Transform

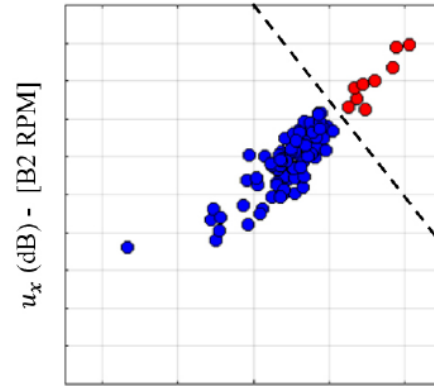
Discrete VSDFT



MODEL LEARNING: GAUSSIAN MIXTURE MODELS



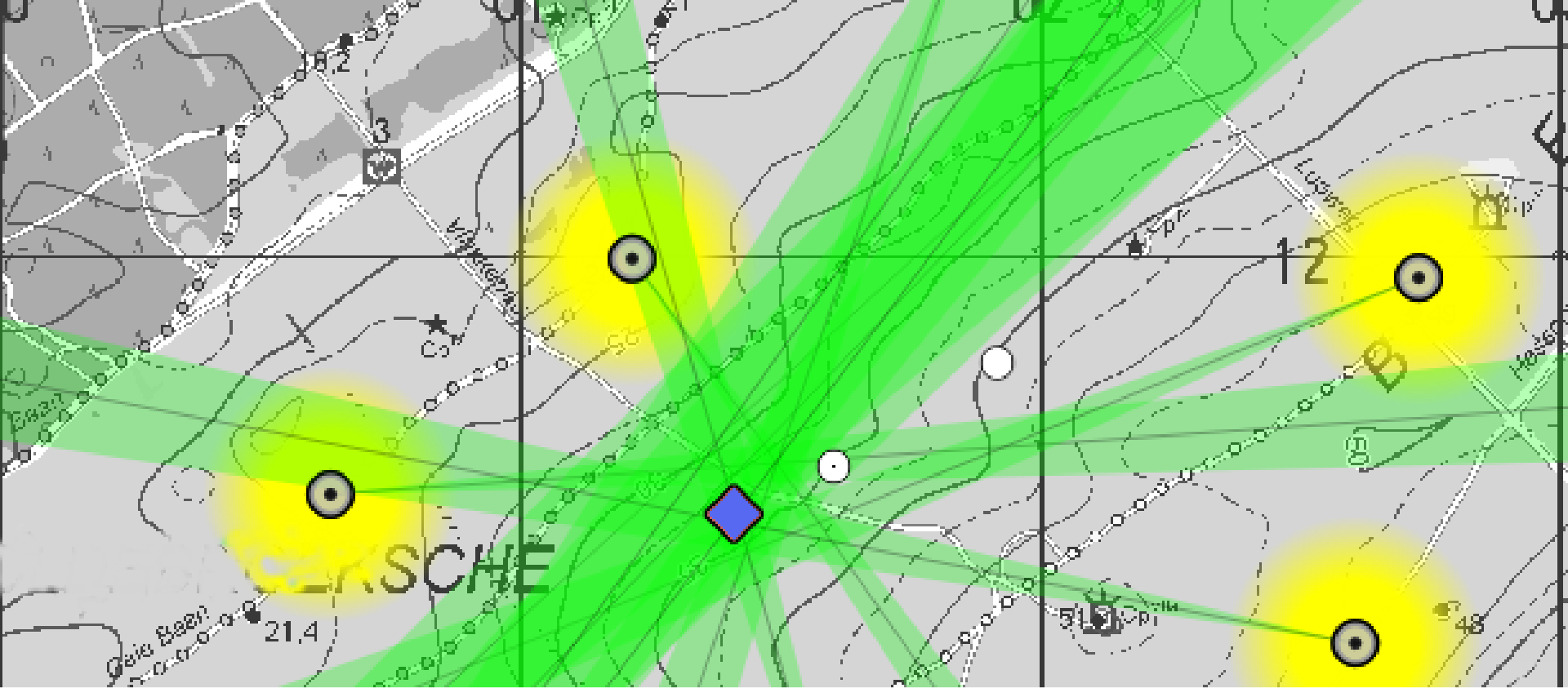
p (dB) - [B1 RPM]



u_x (dB) - [B1 RPM]

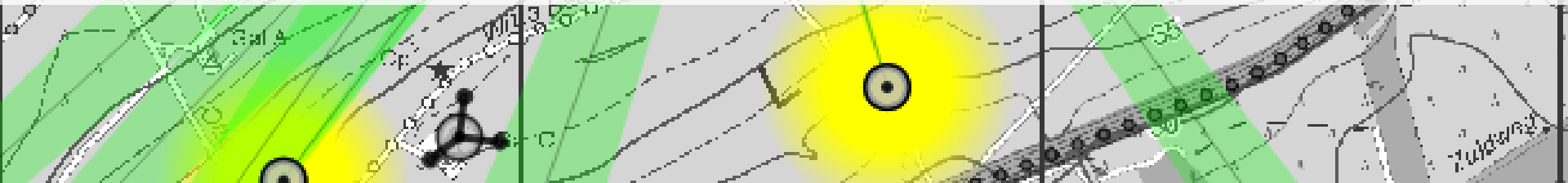
$$p(X | \lambda_m) = \sum_{j=1}^G \omega_j p_j(X)$$
$$p_j(X) = \frac{1}{\sqrt{(2\pi)^{N_f} |\Sigma_j|}} e^{-\frac{1}{2} [(X - \mu_j)' \Sigma_j^{-1} (X - \mu_j)]}$$

- Model the distribution of the samples with the objective to will be able to distinguish GOOD from BAD samples.
- Not many samples available 20/20.
- Neural networks wasn't applicable due sample limitations



OUTDOORS LOCALIZATION

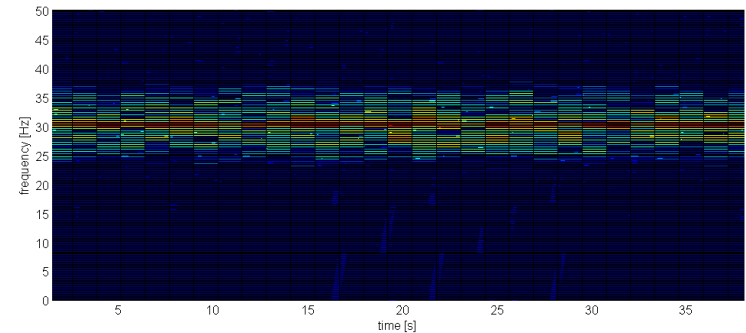
2 Example of application cases



Outdoors localization

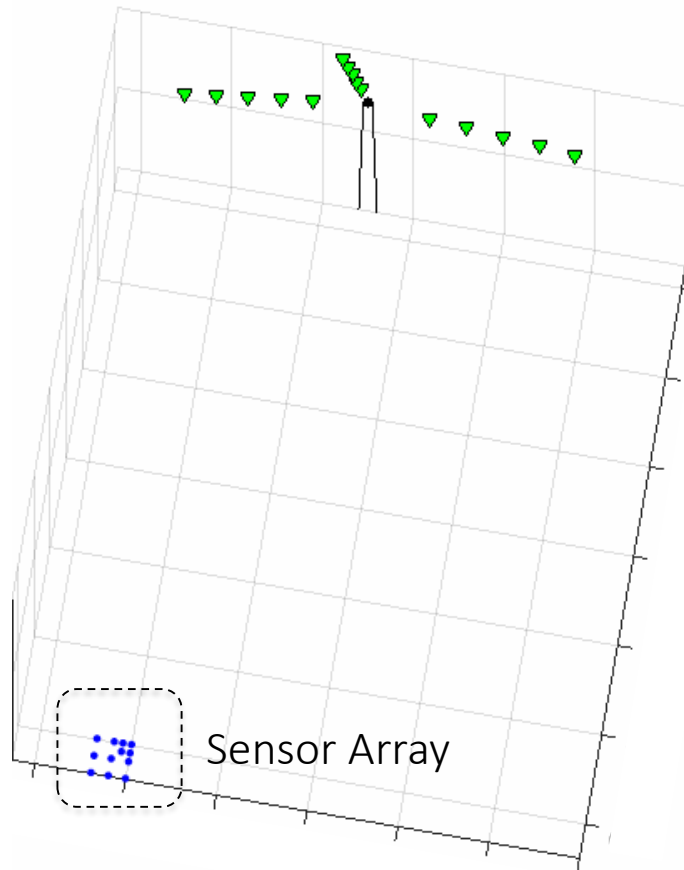
Real time source localization

- ✓ Low frequency noise causes anxiety and insomnia
 - Complaints of about a tonal noise.
- ✓ Deployment of a network of AMMS:
 - Geolocalization of the problem
 - Temporal and spectral analysis
- ✓ Example: Cooling system of a factory in Veendam (Netherlands).
 - Tone located at 30 Hz.
 - The system is being replaced.



Outdoors: Wind Turbine

Moving sources beamforming



Velocity potential can be calculated by convolving the excitation signals with the time-varying propagation functions

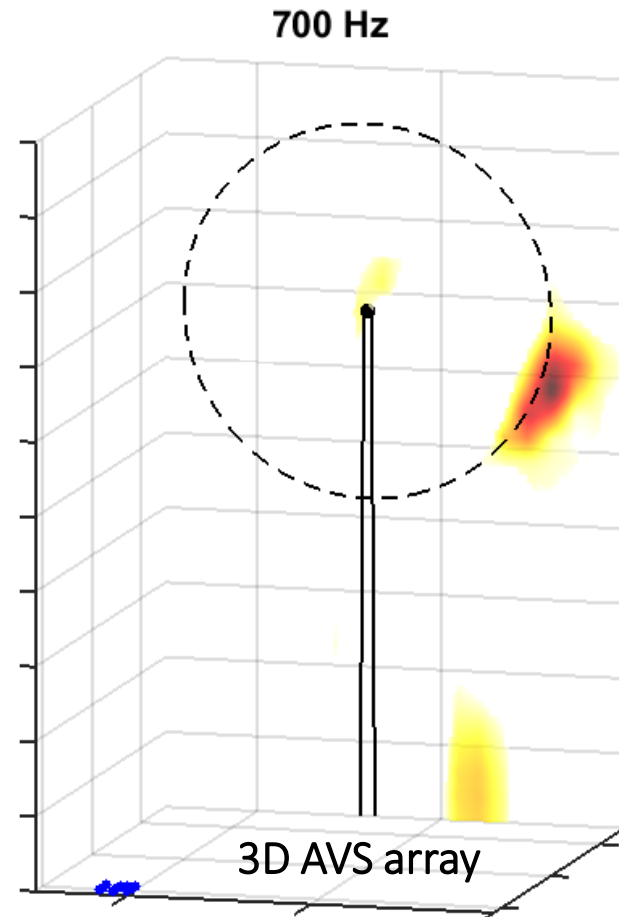
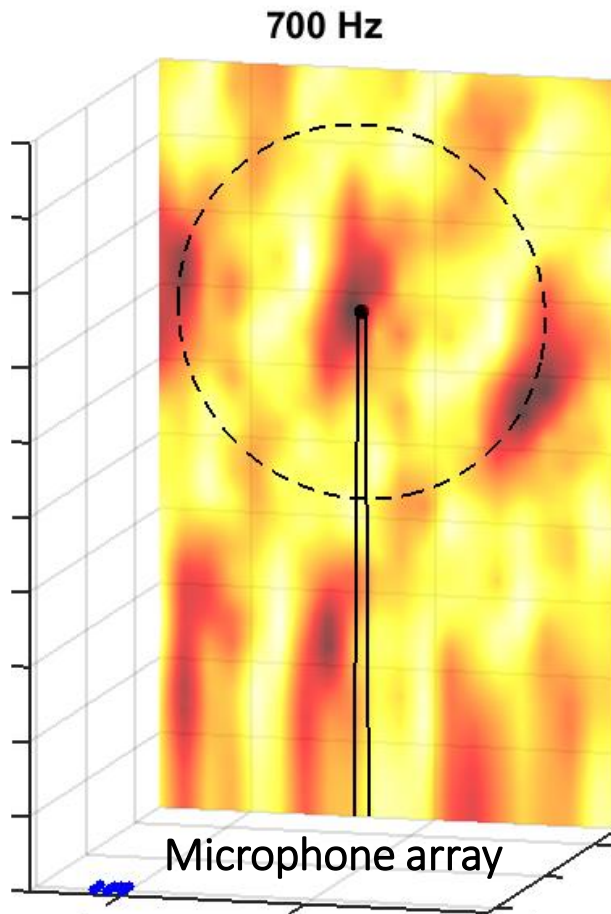
$$\begin{aligned}\Psi_i(\mathbf{x}, t) &= Q_i(\mathbf{x}_0, t) * G(\mathbf{x}, \mathbf{x}_0, t) \\ &= \frac{q_i(t - T)}{4\pi\rho(\|\mathbf{r}_i(t)\| - \mathbf{v}(t - T) \cdot \mathbf{r}_i(t)/c)}\end{aligned}$$

Sound pressure and particle velocity can be directly computed using time and space differentiation

$$\begin{aligned}p(\mathbf{x}, t) &= -\rho \sum_{i=1}^N \frac{\partial \Psi_i(\mathbf{x}, t)}{\partial t} + n(t) \\ \mathbf{u}(\mathbf{x}, t) &= \sum_{i=1}^N \nabla \Psi_i(\mathbf{x}, t) + \mathbf{n}(t),\end{aligned}$$

Wind Turbine: Beamforming results

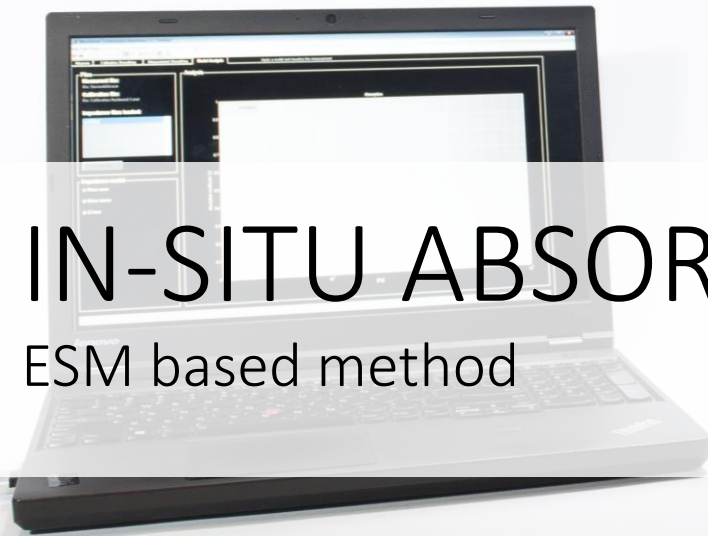
Comparison of microphone array and AVS array : spacing 7 times over Nyquist limit



3

IN-SITU ABSORPTION

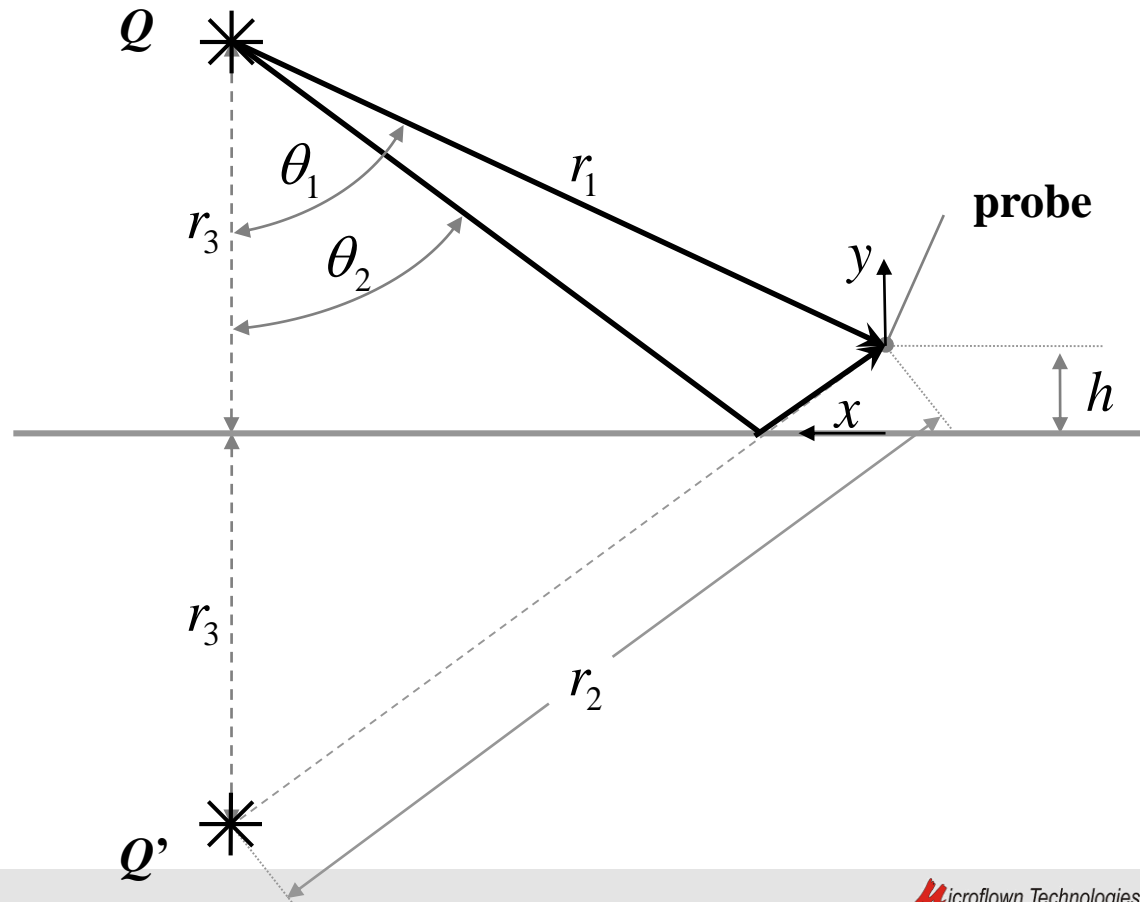
ESM based method



PU in situ method

Motivation

- Extend current in-situ method for impedance estimation to an array of sensors.

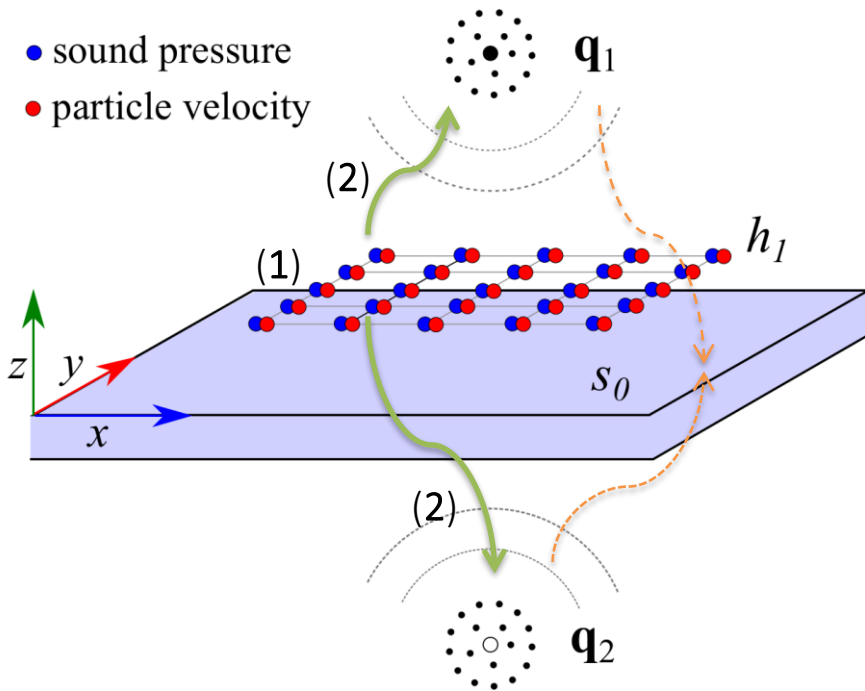


Equivalent Source Method

Array of single later of p-u sensors. Problem definition

Single layer p - u_z

- sound pressure
- particle velocity



Green functions pressure and particle velocity

- $G(\mathbf{r}, \mathbf{r}_i) = e^{-jk|\mathbf{r}-\mathbf{r}_i|}$
- $G^u(\mathbf{r}, \mathbf{r}_i) = \frac{\partial}{\partial z} G(\mathbf{r}, \mathbf{r}_i)$

1. Sound field and sources strength relationship

$$\begin{bmatrix} \mathbf{p}_{h_1} \\ \mathbf{u}_{h_1} \end{bmatrix} = \begin{bmatrix} j\omega\rho\mathbf{G}_{q_1h_1} & j\omega\rho\mathbf{G}_{q_2h_1} \\ -\mathbf{G}_{q_1h_1}^u & -\mathbf{G}_{q_2h_1}^u \end{bmatrix} \begin{bmatrix} \mathbf{q}_1 \\ \mathbf{q}_2 \end{bmatrix}$$

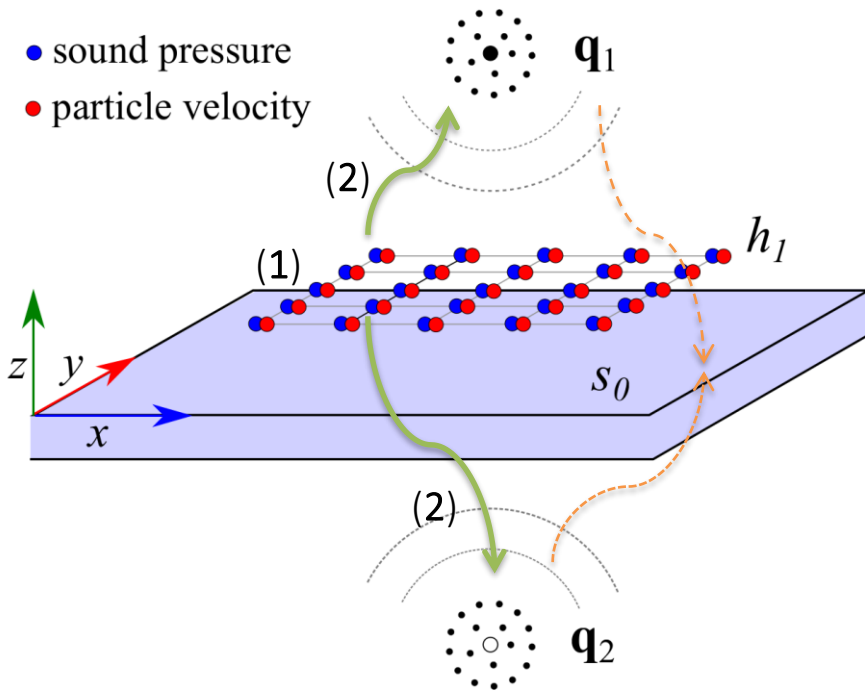
(1) (2)

Equivalent Source Method

Equivalent sources strength estimation. Solving inverse problem.

Single layer $p-u_z$

- sound pressure
- particle velocity



- $$\begin{bmatrix} \mathbf{p}_{h_1} \\ \mathbf{u}_{h_1} \end{bmatrix} = \begin{bmatrix} j\omega\rho\mathbf{G}_{q_1h_1} & j\omega\rho\mathbf{G}_{q_2h_1} \\ -\mathbf{G}_{q_1h_1}^u & -\mathbf{G}_{q_2h_1}^u \end{bmatrix} \begin{bmatrix} \mathbf{q}_1 \\ \mathbf{q}_2 \end{bmatrix}$$

(1) (2)

2. Solving inverse problem for \mathbf{q} (ill-posed)

- $\mathbf{q} = (\mathbf{WG})^+ \mathbf{Wb}$

Where the regularized pseudo-inverse is

- $(\mathbf{WG})^+ = ([\mathbf{WG}^H]\mathbf{WG} + \lambda\mathbf{I})^{-1}[\mathbf{WG}^H]$

And the weighting matrix

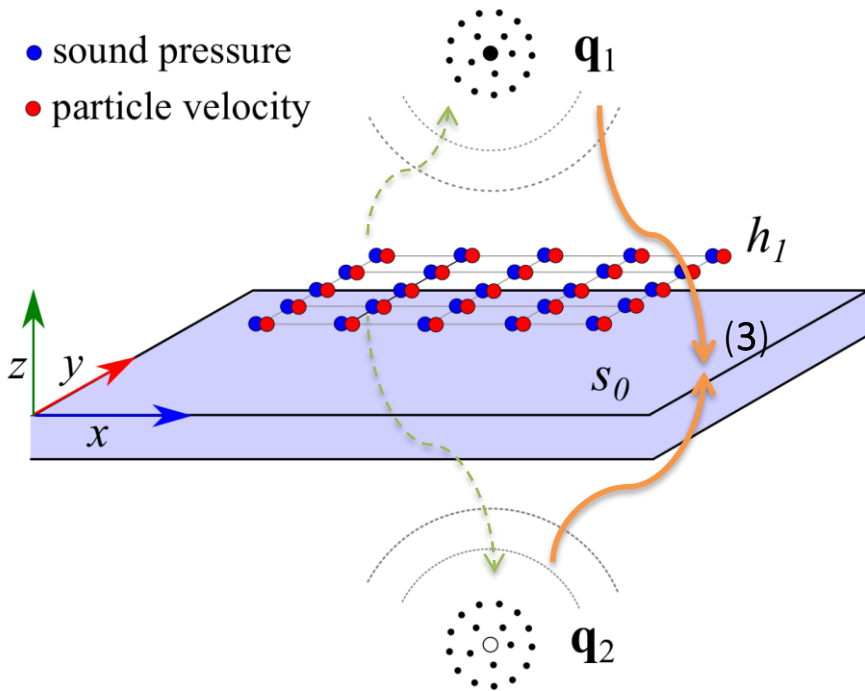
- $\mathbf{W} = \begin{pmatrix} \|\mathbf{p}_h\| & 0 \\ 0 & \|\mathbf{u}_h\| \end{pmatrix}^{-1}$

Equivalent Source Method

Surface impedance and reflection coefficient reconstruction

Single layer p - u_z

- sound pressure
- particle velocity



3a. *Sound field* reconstructed at the *surface* from estimated \mathbf{q}

- $\mathbf{p}_{s_0} = j\omega\rho(\mathbf{G}_{q_1s_0}\mathbf{q}_1 + \mathbf{G}_{q_2s_0}\mathbf{q}_2)$,
- $\mathbf{u}_{s_0} = -(\mathbf{G}_{q_1s_0}^u\mathbf{q}_1 + \mathbf{G}_{q_2s_0}^u\mathbf{q}_2)$

(3)

3b. *Surface impedance* Z_s and *reflection coefficient* \mathbf{R} is computed

- $Z_{s_0} = \frac{1}{N} \sum_{n=1}^N \frac{p_{s_0}^{(n)}}{u_{s_0}^{(n)}}$
- $R_{s_0}(\theta) = \frac{Z_{s_0} \cos \theta - Z_0}{Z_{s_0} \cos \theta + Z_0}$,

(3)

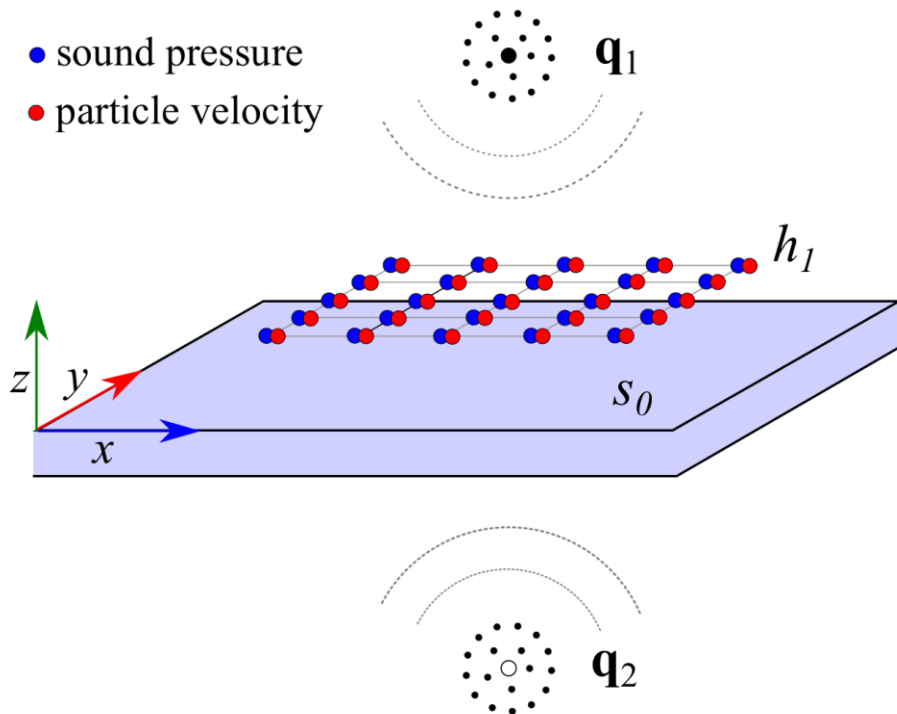
Equivalent Source Method

Comparison: Single layer – Double layer configuration

- Valid for locally reactive samples only: The impedance doesn't change with the angle of incidence)
- Works for different types of sources: monopole / dipole
- Doesn't depend on wave model assumptions like plane wave

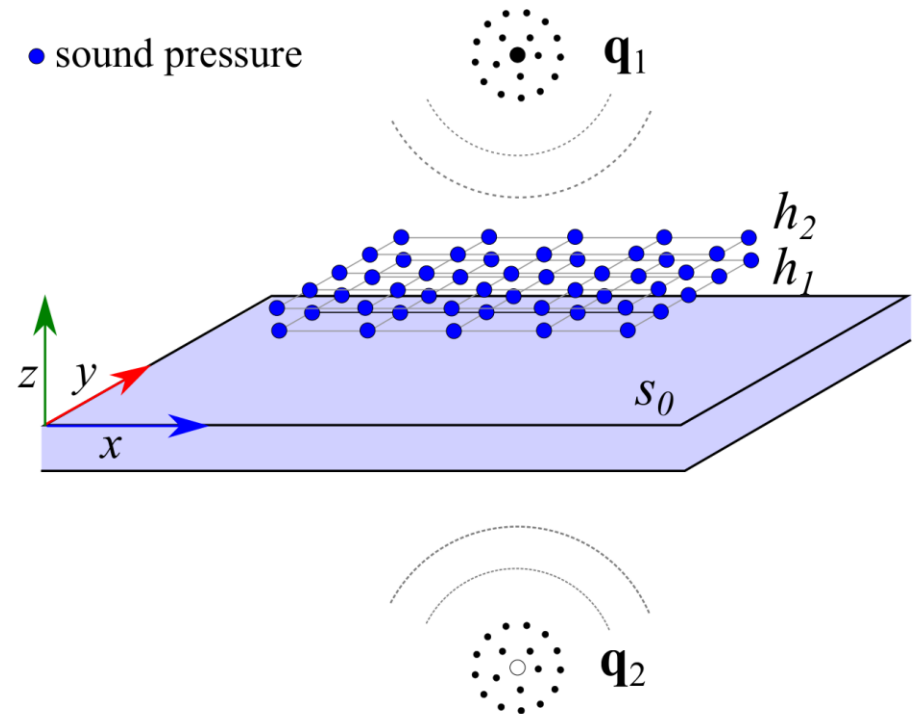
Single layer $p-u_z$

- sound pressure
- particle velocity



Double layer $p-p$

- sound pressure

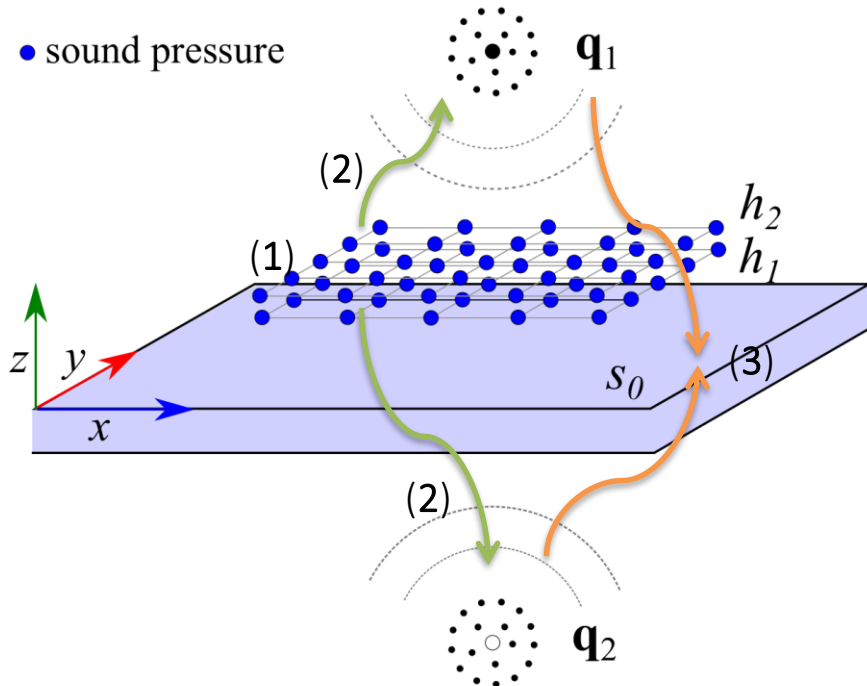


Equivalent Source Method

Double array of pressure transducers. Problem definition

Double layer p - p

• sound pressure



Green functions pressure

- $G(\mathbf{r}, \mathbf{r}_i) = e^{-jk|\mathbf{r}-\mathbf{r}_i|}$

1. Sound field and sources strength relationship

- $$\begin{bmatrix} \mathbf{p}_{h_1} \\ \mathbf{p}_{h_2} \end{bmatrix} = j\omega\rho \begin{bmatrix} \mathbf{G}_{q_1 h_1} & \mathbf{G}_{q_2 h_1} \\ \mathbf{G}_{q_1 h_2} & \mathbf{G}_{q_2 h_2} \end{bmatrix} \begin{bmatrix} \mathbf{q}_1 \\ \mathbf{q}_2 \end{bmatrix}$$

(1)

(2)

Acoustic field and impedance model

Pressure and velocity field model above an impedance plane (Di & Gilbert)

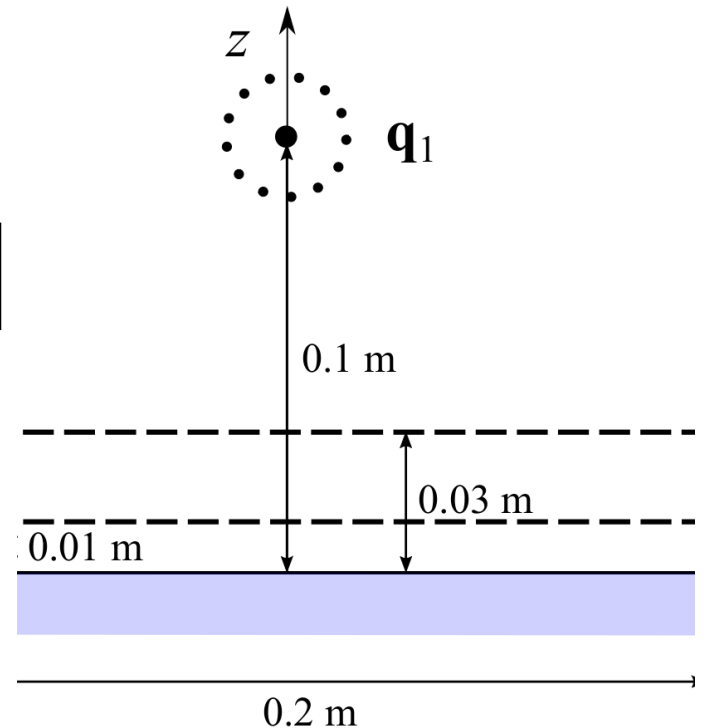
- $$p(\mathbf{r}) = \frac{j\omega\rho Q}{4\pi} \left(\frac{e^{-jk|\mathbf{r}-\mathbf{r}_1|}}{|\mathbf{r}-\mathbf{r}_1|} + \frac{e^{-jk|\mathbf{r}-\mathbf{r}_2|}}{|\mathbf{r}-\mathbf{r}_2|} - 2k\beta \int_0^\infty e^{k\beta q} \frac{e^{-jk\sqrt{d_1^2+(r_{1z}+r_z-jq)^2}}}{\sqrt{d_1^2+(r_{1z}+r_z-jq)^2}} dq \right)$$
- $$u_z(\mathbf{r}) = -\frac{1}{j\omega\rho} \frac{\partial}{\partial z} p(\mathbf{r})$$

Porous media model (Delany and Bazley)

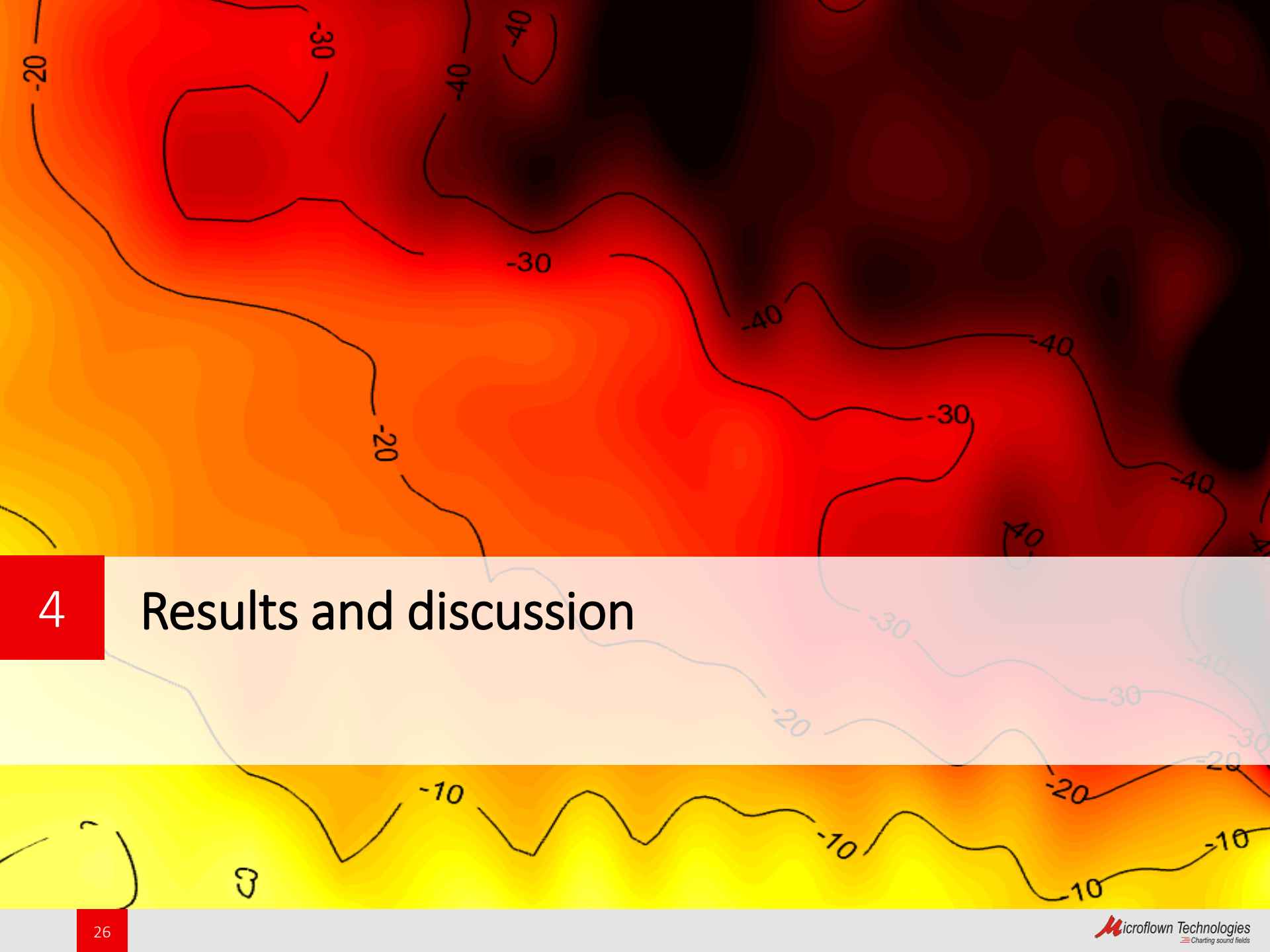
- $$Z_s(f) = Z_0 \left[1 + 9.08 \left(\frac{10^3 f}{e} \right)^{-0.75} - j11.9 \left(\frac{10^3 f}{e} \right)^{-0.73} \right]$$

Relative error in dB

- $$E\{\gamma_{\text{est}}\} = 20 \log_{10} \left(\frac{\|\gamma_{\text{est}} - \gamma_{\text{ref}}\|_2}{\|\gamma_{\text{ref}}\|_2} \right)$$



Sketch of the geometric parameters



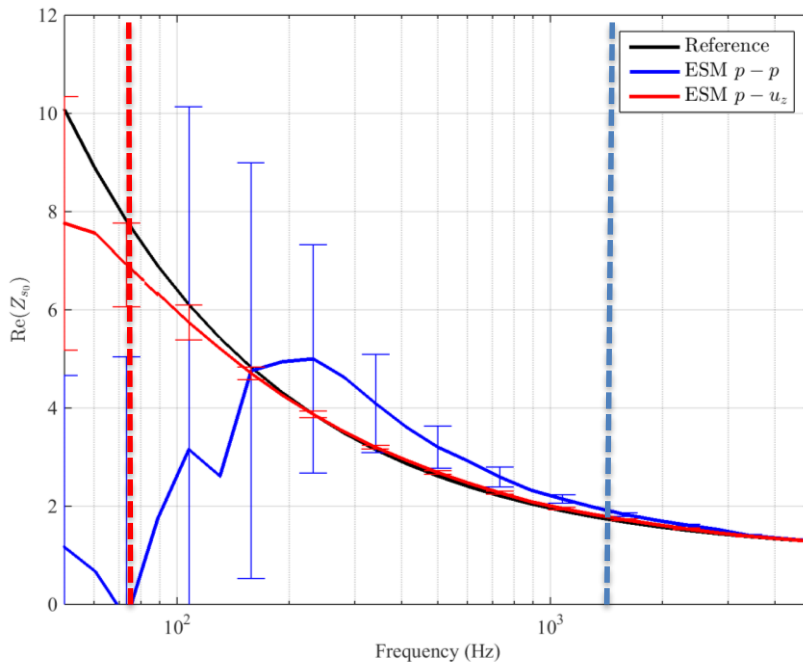
4 Results and discussion

Results and Discussion

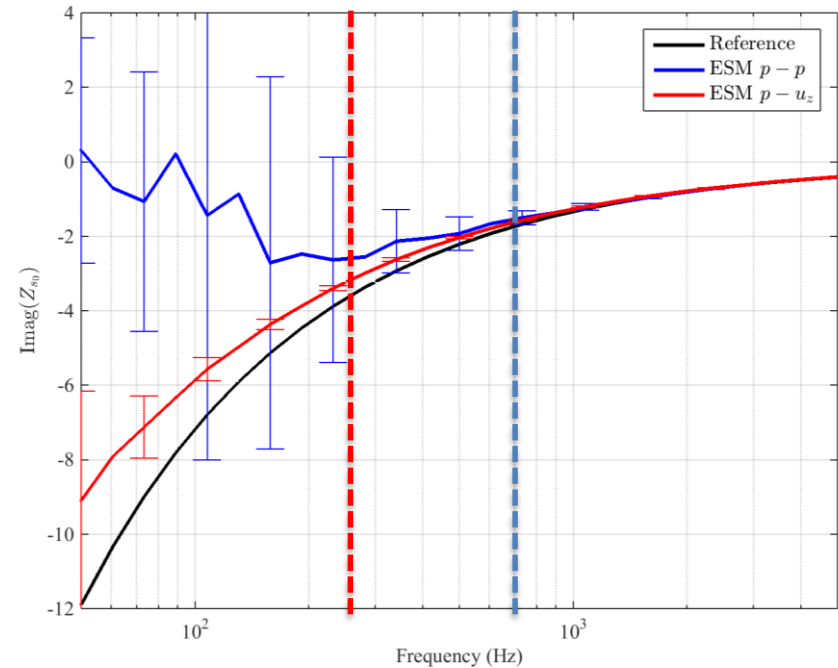
Surface Impedance PU vs PP (SNR 30 dB)

$$Z_{s_0} = \frac{1}{N} \sum_{n=1}^N \frac{p_{s_0}^{(n)}}{u_{s_0}^{(n)}}$$

Real part Surface Impedance



Imaginary part Surface Impedance



< 10 %

< 10 % *Relative error*

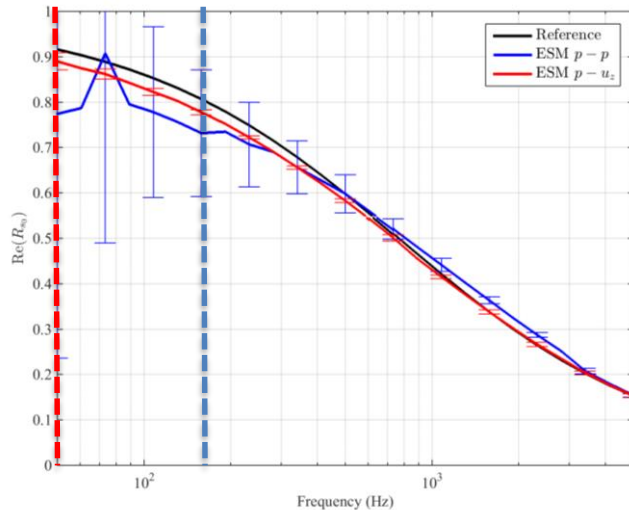
< 10 % < 10 %

Results and Discussion

Reflection coefficient PU vs PP (SNR 30 dB)

$$R_{s_0}(\theta) = \frac{Z_{s_0} \cos \theta - Z_0}{Z_{s_0} \cos \theta + Z_0},$$

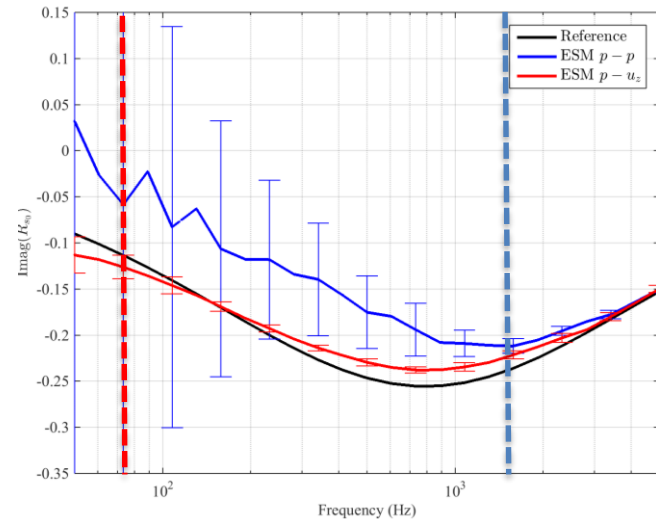
Real part Reflection Coefficient



< 10 % < 10 %

Relative error

Imaginary part Reflection Coefficient



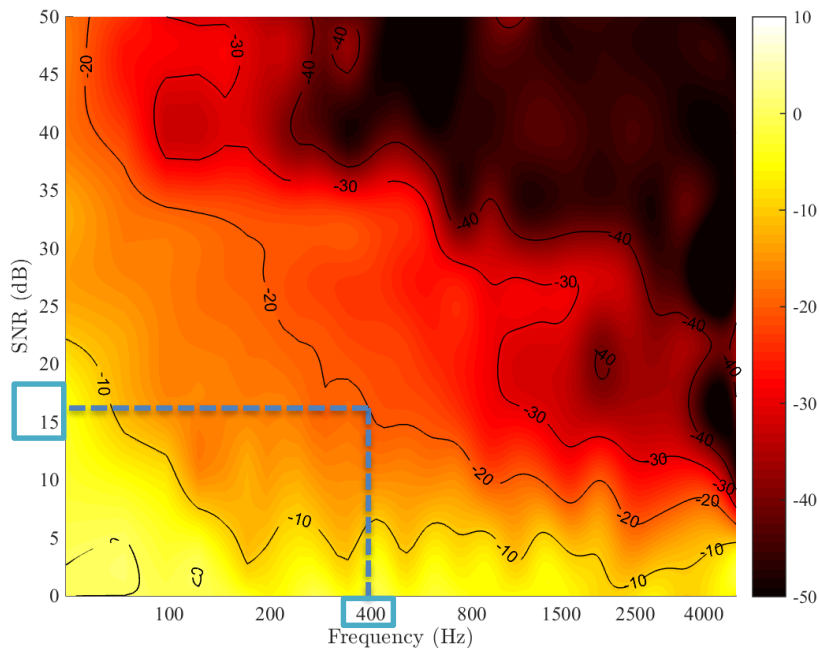
< 10 %

< 10 %

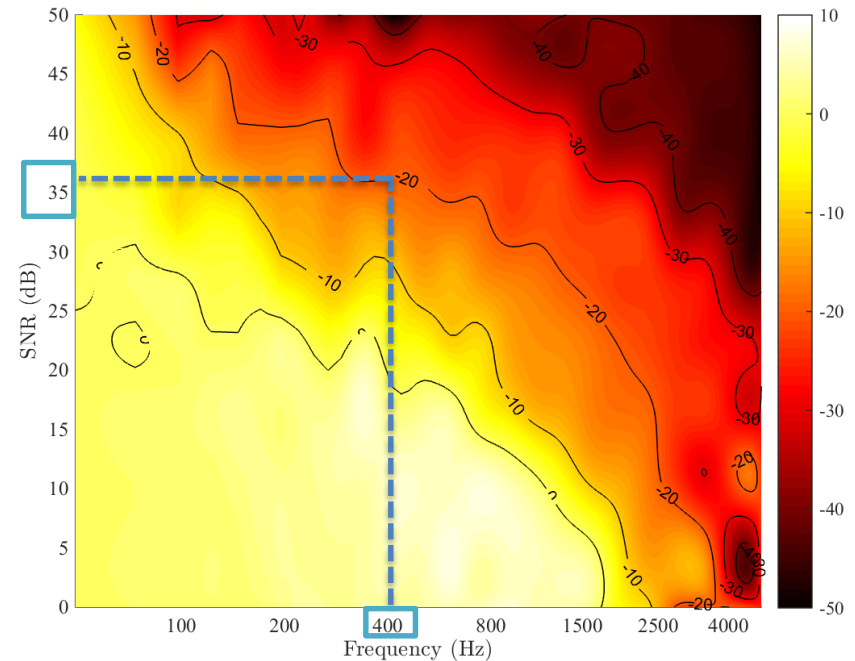
Results and Discussion

Relative error behavior Frequency vs SNR

Single Layer P-U method



Dual Layer P-P method

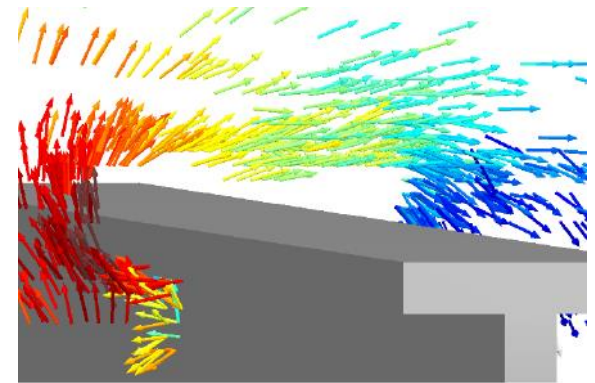
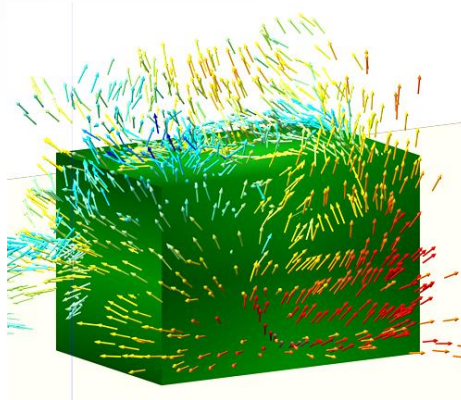
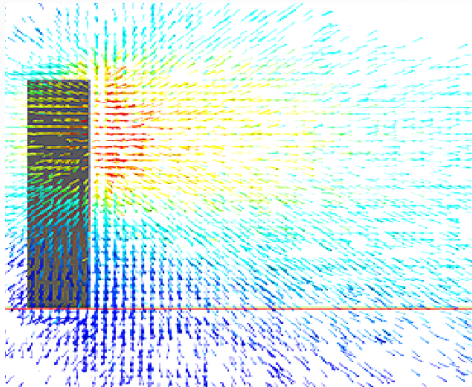


- P-U method: At 400 Hz, < 10 % relative error (-20 dB), -> SNR Needed: 15 dB
- P-P method: At 400 Hz, < 10 % relative error (-20 dB), -> SNR Needed: 35 dB

Conclusions

- Complex **surface impedance** and **reflection coefficient** have been calculated using **ESM** in two configurations: **single-layer** of ***p-u*** probes and a **double** layer of **microphones**.
- The performance of ESM methods across the frequency for different SNR levels were studied.
- **Single layer *p-u*** ESM method has significantly **better performance**, in special in the low frequency range, compared with the **double layer** of **microphones** ESM method.
- In addition, the **single layer *p-u*** is also more robust against noise, achieving **accurate** results with relatively **low levels of SNR**.

Thank you for your attention



Contact us for further information or visit our website



Graciano Carrillo Pousa
carrillo@microflown.com

